Chemical Engineering Journal 162 (2010) 437–447

Contents lists available at ScienceDirect

Chemical Engineering Journal

journal homepage: www.elsevier.com/locate/cej

Review

Halogen element modified titanium dioxide for visible light photocatalysis

Hongqi Sun, Shaobin Wang*, H. Ming Ang, Moses O. Tadé, Qin Li

Department of Chemical Engineering and CRC for Contamination Assessment and Remediation of the Environment (CRC-CARE), Curtin University of Technology, GPO Box U1987, Perth, WA 6845, Australia

ARTICLE INFO

Article history:
Received 22 February 2010
Received in revised form 16 April 2010
Accepted 12 May 2010

Keywords:
Photocatalysis
TiO_2
Halogen modification
Visible light
Organics

ABSTRACT

Halogen elements, i.e. fluorine, chlorine, bromine, and iodine, have attracted intensive interests in modification of TiO_2 for photocatalytic oxidation of organic pollutants under visible light irradiation. Compared to other metal and non-metal elements, halogens show 3-fold advantages, such as improvement of UV activity, various cations or anions for substitution of Ti^{4+} and/or O^{2-} in the TiO_2 matrix, narrowing the band gap of TiO_2 and tuning the band position. In this paper synthesis, physicochemical properties, mechanism of visible response, and photocatalytic activities of halogen modified TiO_2 are reviewed. It is found that introduction of a halogen element into TiO_2 crystals could lead to the enhancement of surface acidity, formation of surface hydroxyl radicals, more active sites, creation of oxygen vacancies or Ti^{3+}, narrowing the band gap and tuning the valence band position. As a consequence, halogen modified TiO_2 exhibited high activity for organics oxidation under visible light radiation in aqueous and gas phases.

1. Introduction

Energy shortage and environmental deterioration have become the major obstacles to the development of economy and society in the past decades. Due to wide applications in solar energy conversion and environmental remediation, photocatalysis using a semiconductor has attracted a considerable attention [1,2]. Titanium dioxide has been intensively investigated as a promising photocatalyst because of its high activity, long-term stability and low cost, etc. Unfortunately, due to its larger band gap (3.2 and 3.0 eV for anatase and rutile, respectively), TiO_2 can only be activated by UV light, which only represents a small portion (3–5%) of sunlight [3]. Driven by the "dream" of utilising solar energy, 1.2×10^5 TW irradiation to the earth, attempts have been making on shifting the absorption threshold of TiO_2 to visible light region, which covers about 42% of solar energy spectrum [4].

Enormous efforts had been devoted to the studies on the red-shift of TiO_2 in the past decades. Many approaches, such as metal ion doping (Fe^{3+} [5], La^{3+} [6], and Ag^+ [7], etc.), semiconductor coupling (TiO_2-CdS [8], TiO_2-Cu_2O [9], and TiO_2-PdS [10], etc.) and dye sensitising (thionines [11], $Ru(bpy)_3^{2+}$ [12], and $RuL_2(NCS)_2$ [13], etc.), have been applied to improve the optical properties of TiO_2. Compared to pure TiO_2, modification of TiO_2 usually resulted in poor thermal and chemical stability and/or lower UV activity. Asahi et al. [14] firstly proposed that doping TiO_2 by non-metal elements, such as nitrogen, would overcome the problems and soon Khan et al. [15] successfully introduced carbon to TiO_2 crystals for water splitting under visible light irradiation. Thereafter, many studies on TiO_2 doped with non-metals, such as nitrogen [16–18], carbon [19–21], sulphur [22], phosphorous [23] and fluorine [24], have been reported. Among these investigations, nitrogen doping has been most extensively studied so far and several reviews have been reported [25–27] in addressing the preparation, effective impurity, activity and mechanism of visible-light response of the nitrogen doped TiO_2. More recently, halogen elements have been proposed as alternative dopants for TiO_2 to obtain visible-light responsive materials, which has not been paid a wide attention.

In fact fluorine, one of halogen elements, was firstly used to improve the UV activity of TiO_2 [28–31]. It was found that fluorine would influence the photocatalytic reactions by changing the interfacial e^-/h^+ transfer, surface charge distribution and substrate-surface interaction, which were attributed to the enhancement of surface acidity, formation of surface hydroxyl radicals, and creation of oxygen vacancies or Ti^{3+}, etc [31]. It is known that the ions with a similar radius to either Ti^{4+} or O^{2-} in TiO_2 crystal can occupy a substituted site. Table 1 shows the ionic radii of halogen elements and it reveals that many halogen ions are able to be doped into TiO_2 crystal to improve the optical property of TiO_2 [32]. Further studies showed that halogen doping could not only narrow the band gap by being lowered to 1.4 eV [33] but also tune the position of the conduction (CB) or valence band (VB)[34]. The studies suggested that halogen doping produces three-fold advantages, i.e. (i) improving UV activity, (ii) providing plenty of dopants especially for co-doping, and (iii) tuning precisely the position of conduction

* Corresponding author. Tel.: +61 8 9226 3776; fax: +61 8 9226 2681.
E-mail address: shaobin.wang@curtin.edu.au (S. Wang).

1385-8947/$ – see front matter © 2010 Elsevier B.V. All rights reserved.
doi:10.1016/j.cej.2010.05.069

Table 1
Ionic radius of halogens, Ti^{4+} and O^{2-} in TiO_2 matrix [32].

Element	Anion radius (nm)	Cation radius (nm)
Ti		Ti^{4+} (TiO_2): 0.068
O	O^{2-}(TiO_2): 0.124	
F	F^-(HF): 0.133	F^{7+} (FO_4^-): 0.008
Cl	Cl^-(HCl): 0.181	Cl^+(ClO^-): 0.130; Cl^{3+}(ClO_2^-):0.105; Cl^{5+}(ClO_3^-):0.012; Cl^{7+}(ClO_4^-): 0.020
Br	Br^-(HBr): 0.196	Br^+(BrO^-): 0.106; Br^{3+}(BrO_2^-):0.082; Br^{5+}(BrO_3^-):0.059; Br^{7+} (BrO_4^-): 0.039
I	I^-(HI): 0.220	I^+(IO^-): 0.170; I^{3+}(IO_2^-):0.139; I^{5+}(IO_3^-):0.062; I^{7+}(IO_4^-): 0.050

or valence band, which is relating to the reduction and/or oxidation ability of the photogenerated carries. Thus, halogen doping offers flexible ways to control the activity, the optical property and the electronic structure of TiO_2 photocatalyst [35]. In the past decade, many investigations have been conducted while no review in this topic has been reported. This paper will discuss the synthesis of halogen modified TiO_2, summarise and compare their physicochemical structure and properties, and discuss the mechanism of visible-light response as well as their activities in degradation of organics. The authors believe that this review will be very helpful for design, synthesis and development of novel photocatalysts, as well as providing insights into the mechanism of visible-light response from ion doping.

2. Synthesis of halogen modified TiO_2 photocatalysts

Many approaches have been successfully developed to prepare halogen modified TiO_2 photocatalysts, including hydrolysis, sol–gel synthesis, hydrothermal preparation, pyrolysis, ion implantation, chemical vapour deposition (CVD), electrochemical anodisation, and thermal plasma oxidation. Here we discuss some typical synthesis processes and the interest will focus on the bonding of halogens to TiO_2 crystal structure.

2.1. Hydrolysis

Hydrolysis of an inorganic Ti-precursor is a traditional approach for preparation of nano-sized TiO_2 materials [36,37]. The basic procedure includes hydrolysis of the Ti-precursor, formation of precipitate with the composition of $TiO_2 \bullet nH_2O$ and calcination of the precipitate [36]. With addition of the donors, e.g. NH_4F or HIO_3, in the hydrolysis process, F-doped and I-doped TiO_2 were synthesised [24,38–40]. This method is simple in changing the donors and selecting the doping ions, while generally resulting in material aggregation [24,38,40]. Yu et al. [24] recently have reported synthesis of a mesoporous structured F-doped TiO_2 using this technique, but no other studies have reported the similar structure for doped TiO_2 photocatalysts.

2.2. Sol–gel process

The sol–gel process also affords simplicity in controlling the doping level and particle size by changing the experimental conditions, such as hydrolysis rate, solution pH and solvent system [27]. A typical sol–gel process for halogen-TiO_2 involves the hydrolysis of Ti-precursors (e.g. titanium (IV) tetraisopropoxide, tetrabutyl titanate, and tetraethyl orthotitanate) in a mixture of ethanol and water, with the addition of halogen element donors, such as NH_4F, HF, CF_3COOH, NH_4Br, and HIO_3, etc. In the sol–gel process of pure TiO_2, TiO_2 usually was derived from the reactions of hydrolysis and polycondensation of titanium alkoxides, $Ti(OR)_n$ to form oxopolymers rather than an oxide network. The reaction scheme is usually written as follows [41].

Hydrolysis

$$M(OR)_n + H_2O \rightarrow M(OR)_{n-1}(OH) + ROH \quad (1)$$

Dehydration

$$M(OR)_n + M(OR)_{n-1}(OH) \rightarrow M_2O(OR)_{2n-2} + ROH \quad (2)$$

Dealcoholation

$$M(OR)_n + (n/2)H_2O \rightarrow MO_{n/2} + nROH \quad (3)$$

Generally the halogen doping could be controlled by changing solution composition (Eq. (1)), in which the donors, e.g. F^- [42–46], Br^- [47], or I_2 [48], were introduced to partially replace –OH and be incorporated in the network of –Ti–OH. Then, the gels would experience a calcination process which in most cases will determine the doping level, crystal phase, and particle size. Although the detailed mechanism of ion doping processes has not been fully elucidated, the doped elements possibly are, as proposed by Sun et al. [3], incorporated via crystal transformation of TiO_2 from amorphous to anatase or rutile. It is noted that, due to the substitution of exterior radicals –OH, the crystal phase of TiO_2 would be determined by both the calcination and sol composition. Pure anatase [42–45] or mixed crystals of anatase and rutile [45–48] were found in halogen modified TiO_2. Furthermore, the doping level can only be empirically controlled due to the oxidation of non-metal elements during the calcination. Usually the morphology of doped TiO_2 via the sol–gel shows a sphere-like structure being rough and agglomerated [43], and sometimes void structure at higher temperatures [43,48].

2.3. Hydrothermal synthesis

Hydrothermal synthesis has been widely used in the preparation of highly dispersed, and shape-controlled (i.e. nanotubes, nanorods, and nanowires) nanocrystal TiO_2 [49–51]. The dopants and characteristics of TiO_2 could be precisely controlled by changing the physicochemical parameters of the synthesis system, such as temperature, pH, reactant species and concentration [49]. Hydrothermal synthesis has been applied to prepare F-doped, Cl-doped, Br-doped and I-doped TiO_2 by many research groups [33,52–57]. In morphology, halogen doped TiO_2 via a hydrothermal method could be nanoparticle [33,52,54,55,57], nanorod [56] and microsphere [53]. In terms of microstructure, mesopores or nanopores were found in the halogen doped TiO_2 materials [52–54] which have a lager specific area from 100 to 170 m^2/g and a crystalline size between 5 and 20 nm. If controlling aqueous reactants and heating, the crystal phases could be obtained in pure anatase [53,57], rutile [56], and mixture [33,52,54,55].

2.4. Spray pyrolysis

Gaseous phase spray pyrolysis is widely used on the industrial scale to produce ceramic materials [58] with a considerable variety of particle morphologies, sizes, and compositions. Using H_2TiF_6 as both Ti and F precursors, Li et al. [59,60] synthesised F-doped TiO_2 powders via the spray pyrolysis. The as-prepared F-doped TiO_2

Table 2
Chemical states and binding energies of doping halogen ions in TiO_2.

Ion	Orbital	Compound	Binding energy (eV)	Ref.
F^-	F 1s	$TiO_{2-x}F_x$	688.0	[24]
F^-	F 1s	$TiO_{2-x}F_x$	687.8	[60]
		$TiOF_2$	685.3	
F^-	F 1s	$TiO_{2-x}F_x$	688.0	[46]
		$TiOF_2$	685.4	
		TiF_4	684.3	
F^-	F 1s	$TiO_{2-x-y}F_xN_y$	688.5	[64]
		Surface fluorine	685.5	
Cl^-	Cl $2p_3$	$TiO_{2-x}Cl_x$	198.0	[56]
I^{5+}	I $3d_5$	$Ti_{1-x}I_xO_2$	627.5	[38]
I^{5+}	I $3d_5$	$Ti_{1-x}I_xO_2$	624.5	[54]
I^-	I $3d_5$	Surface I^-	619.0	[65]
I^{7+}		Surface IO_4^-	624.0	
I	I $3d_{3/2}$	I_2	620.1	[33]
			631.6	
I^{5+}	I $3d_{5/2}$	$Ti_{1-x}I_xO_2$	623.6	
			635.0	

possessed the morphology of spherical particle with an average particle diameter of 0.45 μm. With increasing the temperature, the rutile contents would be increased with increased crystallite size from 13 to 30 nm and the decreased BET surface area from 35 to 10 m^2/g. The F-doped TiO_2 showed higher photocatalytic activity under both UV and visible light when compared to a reference of P25 TiO_2.

In synthesis of modified TiO_2, many other approaches have also been employed to obtain halogen modified TiO_2 photocatalysts, e.g. ion implantation [61], electrochemical anodisation [62], and radio frequency thermal plasma oxidation [63]. In general the equipments used in the above synthesis routes are expensive, and the preparation conditions are neither easy to control nor flexible to change doped ions.

3. Physicochemical properties of halogen modified TiO_2

3.1. Chemical nature of doped halogen elements in TiO_2

The chemical state and doping level of halogen elements in TiO_2 are the key features in halogen modified TiO_2 photocatalysts. X-ray photoelectron spectroscopy (XPS) provides fundamental information regarding the composition, electronic structure, and environment of each element on a surface up to a few nanometres in depth [27]. Therefore, for nano-scaled halogen doped TiO_2, XPS would figure out a panoramic view of the chemical nature of the materials. With a comprehensive analysis of the chemical states of dopants together with the chemical composition of pure TiO_2 (including ionic radii of Ti^{4+} and O^{2-}), the modified types, i.e. substituted doping, interstitial doping, and chemical and/or physical adsorption could be then determined. With the understanding of the chemical states, the electronic structure, band structure and optical property could be studied. Table 2 lists the binding energies of various halogen modified TiO_2 samples from previous reports.

Fluorine is the most active element among all halogens and it is easy to obtain an electron to form an ion with chemical state of −1. Yu et al. [24] used XPS to measure the chemical states of the doping F and found that the F 1s could be assigned to two components. The major contribution was the F in solid solution $TiO_{2-x}F_x$ and the minor one was from the F^- ions physically adsorbed on the surface of TiO_2. Li et al. [60] and Ho et al. [53] proposed that the F 1s could be attributed to the F-atoms which were doped into the oxygen sites of the TiO_2 crystal lattice in their investigations. Todorova et al. [45] found three F species in F doped TiO_2 by XPS, the peak at 684.3 eV indicated that the fluorine was presented mainly as TiF_4 and/or physically adsorbed F^- on the surface. The second at 685.4 eV could be related to $TiOF_2$ structure and the tail at 688 eV to the F in solid solution $TiO_{2-x}F_x$. All these studies suggested that the F-atoms in F-doped TiO_2 were mainly at the crystal O sites with a chemical state of −1. Theory studies using density function theory (DFT) have also suggested that it is energetically more favourable for F to substitute O sites in TiO_2 crystal matrix [35].

In general, Cl will also occupy the O sites of TiO_2 matrix when it is introduced to TiO_2 crystal, and is in the chemical state −1. Xu et al. [56] reported the observation of a Cl peak around 197 eV in XPS and attributed it to Cl $2p_3$. Due to larger atomic radius of Cl (1.81 Å) than O (1.32 Å), the cell parameters would change with the increase in dopant concentration [56].

Iodine modification is more complex in chemical structure different from other halogen modified TiO_2 systems. Iodine would produce various chemical states, e.g., −1, 0, +5, and +7. The varying chemical states account for the different occupied sites of doping iodine in TiO_2 matrix, leading to variation of band structures and optical properties of TiO_2.

Iodine doped TiO_2 with visible-light response was firstly prepared by Hong et al. [38]. They found that the iodine doped TiO_2 prepared by a hydrolysis method showed a high efficiency for decomposition of phenol under visible light irradiation. The high-resolution XPS spectra showed a I $3d_5$ peak at the binding energy of 627.5 eV, which was aroused from I^{5+} (ionic radius of 0.62 nm) substitution of Ti^{4+} (ionic radius of 0.64 nm). It was also suggested that the iodine source may control the chemical states of the iodine dopant, for instance, I^{5+} had also been observed by Liu et al. [54], Tojo et al. [33], and He et al. [39] in iodine doped TiO_2 using HIO_3, the same result as Hong et al. [38]. The XPS spectra showed the similar pattern to that of Hong et al. [38] while the band gap energies varied at a large range from 1.40 to 2.50 eV [33,54]. Also, surface iodine species had been found in I-doped TiO_2 samples, which were dispersed on the particles [64,65].

Due to the unique chemical activity of halogens, these dopants intend to more easily occupy a substituted site in TiO_2 matrix than the well-known dopant of nitrogen. The doped nitrogen would be generally detected by XPS at the binding energy of either 396 eV or 400 eV [16]. The former binding energy has been recognised as the result of substitution of lattice oxygen by nitrogen, while the latter one was resulted from surface NO_x species [16]. Formation of Ti-N bond may significantly reduce the band gap energy, but surface nitrogen-containing species produces less effect on the change of the band gap. During the synthesis, the formation of Ti-N only occurred in an energy extensive process, such as oxidation of Ti-N, heating under NH_3 atmosphere, sputtering, etc., other than mild preparation process like wet chemistry [17]. In this regard, halogen modification brings out merits since wet processes can easily produce substituted doping. Therefore, the halogen modified TiO_2 from the cost-effective synthesis can respond visible light at a longer wavelength than the nitrogen-doped TiO_2. Furthermore, the multivalence of halogen elements could make it feasible for tuning the desired position of CB or VB by band gap engineering. Anion and cation doping though could be obtained in sulfur doping [3], however, UV activity was generally found to be hindered [66].

3.2. Surface features

Halogen ions could change the surface properties of TiO_2 by altering the chemical composition (oxygen vacancy, surface hydroxyl radical, and Ti^{3+}), morphology, surface acidity, surface area, and photoinduced hydrophilicity. On the other hand, the photocatalytic efficiency depends on the competition between surface charge transfer process and electron–hole recombination. Thus the photocatalytic efficiency was significantly affected by TiO_2 surface defect as well as the radicals [24].

Hattori et al. [28] prepared a highly photoreactive sol–gel TiO_2 film on the soda-lime (SL) glass substrate with a SiO_2 film containing fluorine. They found that HF promoted the oxidation of the gel-TiO_2 film to reduce surface oxygen vacancy and that F^- ions decreased the rate of the h^+/e^- recombination as the result of the filling of oxygen vacancy, contributing to the significant enhancement of activity. However, more studies have proven that the incorporation of F^- led to the formation of O vacancies [44,45,53,59–61,67]. In photoluminescence (PL) spectra, Li et al. [60] found two kinds of oxygen vacancies (F and F^+ centres) were formed by F-doping, and that the visible-response photocatalytic activity for F-TiO_2 powders was ascribed to the creation of these oxygen vacancies. Comparison with the activity of P25, they also suggested that the high photocatalytic activity was due to several beneficial effects produced by F-doping, e.g. enhancement of surface acidity, creation of oxygen vacancies, and increase of active sites [59]. Czoska et al. [44] further found that, besides the oxygen vacancies, F-doping could also induce the formation of reduced Ti^{3+} centres that localise the extra electrons needed for charge compensation.

Photo-induced hydrophilic properties had also been observed on F-doped TiO_2. Tang et al. [68] found that fluorination remarkably increased the adsorption of polar molecules, including water and some organics. They attributed this property to the enhancement of surface acidity, and the formation of surface hydroxyl radicals, which are beneficial for both photocatalytic oxidation and hydrophilicity. More recently, Chen et al. [67] observed that the surface fluorination increased the adsorption of rhodamine B (RhB) on porous TiO_2 film and enhanced the photocatalytic degradation of RhB. Also, under UV light irradiation, the water contact angle of the porous F-TiO_2 film decreased to 5.1° in 90 min.

Chlorination also significantly influences the surface properties of TiO_2. Li et al. [63] found that Cl-doping induced the formation of oxygen vacancies not only in anatase but also in rutile crystals. Moreover, excessive surface Ti^{3+} ions were found, which may act as surface recombination centres for h^+/e^- and accordingly suppress the photocatalytic activity. However, Xu et al. [56] suggested that Cl-doping increased the surface acidity, created surface defect, and produced more $OH^\bullet$ radicals, which enhanced the photocatalytic activity.

The substitution of Ti^{4+} with I^{5+} would induce the formation of surface Ti^{3+}, and the existence of the surface Ti^{3+} was suggested to suppress the recombination of the electron–hole pairs [38]. Tojo et al. [33] found that the amounts of surface $OH^\bullet$ groups were significantly decreased by I-doping into TiO_2. With the results of ATR-FTIR, they suggested that the I-TiO_2 surface was more hydrophobic than undoped TiO_2.

The formation of surface Ti^{3+} was observed to occur in F-doping [44], Cl-doping [63] and I-doping samples [38], while its contribution to photocatalytic activity has not been clearly understood. For instance, some researchers suggested that the surface Ti^{3+} would reduce the recombination rate of photoinduced h^+/e^- pairs leading to an enhancement of photoactivity [24,38,69,70]. That is plausible because the Ti^{3+} surface species may trap the photogenerated electrons and transfer the electrons to adsorbed O_2 on the surface, resulting in the reduction of the h^+/e^- recombination [24,69,70]. However, some other studies reported that the surface Ti^{3+} could be recombination centres and consequently reduce the photocatalytic efficiency [63,71]. In those investigations, it was found that the 3d states of Ti^{3+} would form defect energy levels of 0–0.35 eV, lower than the conduction band and the new energy levels would act as the recombination centres [72,73]. Nevertheless, in most cases of h^+/e^- recombination either in reducing or increasing rate, the variations of Ti^{3+} amount and the effects of other dopants were not taken into account. The inconsistencies were possibly attributed to the different Ti^{3+} concentrations derived from sample synthesis even if the rate change was not due to the presence of other dopants. The studies on Ti^{3+} species in pure TiO_2 might help address this issue more clearly. Using DFT models for pure TiO_2, Takeda et al. [74] reported that no new energy levels would be formed in the band gap at lower Ti^{3+} concentration, while the energy levels would be produced at higher concentration. The conclusion was experimentally proven by Scotti et al. [75]. The controversy on the oxygen vacancies in photocatalysis may also be the same reason since the oxygen vacancies are closely related with Ti^{3+} [44,59,60,63], and their concentrations were varying in different samples during synthesis [74]. Therefore, further research is highly required to elucidate the role of Ti^{3+}.

3.3. Optical properties

The optical properties of photocatalysts generally play a significant role in visible light photocatalysis. UV-visible diffuse spectra (UV-vis) can directly reveal the visible absorption of halogen modified TiO_2 photocatalysts. Since TiO_2 is an indirect band-gap material, the intercept of the tangent to the plot of UV-vis spectrum will give a good approximation for the band gap energy of modified TiO_2 photocatalysts.

Fig. 1 illustrates UV-vis spectra of pure and doped TiO_2. Fig. 1(A) shows the optical properties of pure and nitrogen-doped TiO_2, which were used as references to halogen element doped TiO_2. It is found that N-doping slightly decreases the band gap of TiO_2, while creates a new absorption band in visible region [17]. Fig. 1(B) suggests that F-doping can hardly change the absorption spectra of TiO_2 [60]. More surprisingly, no absorption bands in visible region can be created by F-doping. These results have been confirmed by other studies [44–46,53]. Yamaki et al. [61] theoretically studied the effect of F-doping on the absorption spectra and concluded that, when TiO_2 is doped with F, the localised levels with a high density will appear below the valence band. Moreover, these levels are composed of F 2p state without any mixing with the valence or conduction band; consequently, they are not expected to contribute to the optical absorption spectra of TiO_2.

Fig. 1(C) displays the plots of $(\alpha h\nu)^{1/2}$ versus the energy of absorbed light and diffuse reflectance absorption spectra of Cl-doped TiO_2 and P25 [56]. Cl-doping shifts the absorption of TiO_2 to visible region, and the band gap of Cl-doped TiO_2 is 2.99 eV. A similar red-shift for Cl-doping was also observed by Li et al. [63].

I-doping would greatly improve the absorption property of TiO_2, as shown in Fig. 1(D) [33]. The absorption in visible region observed in the I-TiO_2 was much stronger than those of pure TiO_2 and N-TiO_2 powders and the band gap of the I-TiO_2 was roughly estimated to be 1.4–2.2 eV. The red-shift from I-doping is also much better than that of F- or Cl-doping. This conclusion can be supported by other studies. Hong et al. [38] found that the absorption of iodine-doped TiO_2 samples showed drastic and stronger photoabsorption in the range of wavelengths between 400 and 550 nm compared to P25 and pure TiO_2. The absorption edge of iodine-doped TiO_2 is 441 nm, corresponding to a band gap of 2.81 eV.

When evaluating the absorption change from doping halogens, we found that the range and intensity become better in visible region with increased molecular weight of elements from fluorine to iodine. Besides the influence of chroma from possible physical/chemical adsorption of certain molecules, as found in nitrogen doped TiO_2 [14], another plausible reason is that the formation of halogen-containing groups becomes easier with increasing atomic number in halogen family. For instance, iodine has proven to be the best dopant for creation of lower band-gap TiO_2 by mild synthesis [33]. It is noteworthy that visible light absorption is the basis for inducing photoactivity, however, the strong absorption does not justify a better activity due to other influencing factors.

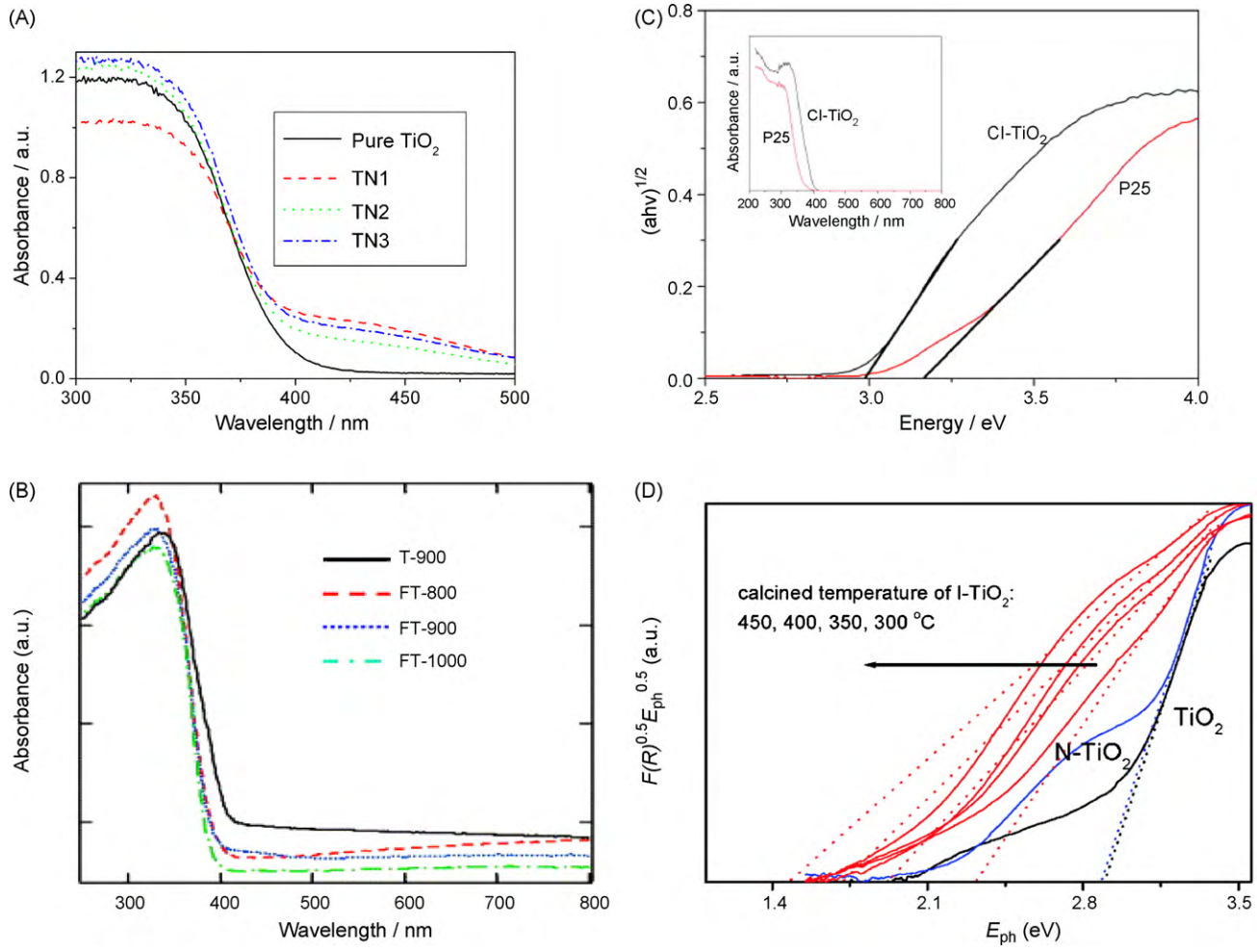

Fig. 1. UV-visible diffuse spectra of N, F, Cl and I doped TiO_2. (A) Absorption spectra of N-doped TiO_2 and pure TiO_2 [17]; (B) absorption spectra of F-doped TiO_2 and pure TiO_2 [60]; (C) plots of $(\alpha hv)^{1/2}$ versus the energy of absorbed light and diffuse reflectance absorption spectra (inset) of Cl-doped TiO_2 and P25 [56]; (D) plots of the square root of the Kubelka-Munk (F(R)) versus the photon energy of I-doped TiO_2, N-doped TiO_2 and pure TiO_2 [33].

4. Mechanism of visible-responsive photocatalysis

4.1. Crystal and band structure of TiO_2

Two crystal structures of TiO_2, rutile and anatase, are generally used in photocatalytic reactions, with anatase showing a superior efficiency [76–78]. Recently, mixed-phase TiO_2 photocatalyst has been found to show higher activity than that of single rutile or crystal titania [79,80]. In TiO_2 crystals, each Ti^{4+} ion is surrounded by an octahedron of six O^{2-} ions. The bulk structure of both anatase and rutile crystals can be described using TiO_6 octahedra. The difference in the crystals of rutile and anatase is the connection type of the octahedron. Each octahedron in rutile crystals connects with two sharing edges and eight sharing corners while an octahedron connects with four edges and four corners in anatase. Moreover, the distortion of the TiO_6 octahedron in anatase crystal is significantly larger than that of rutile [81]. These differences in bulk crystal structure will eventually be embodied in the crystal surface structure on which a photocatalytic reaction occurs.

TiO_2 semiconductor possesses a void energy region where no energy levels are available to promote recombination of electrons and holes produced by photoactivation under light irradiation. The electronic structure of nearly perfect TiO_2 surface is essentially identical to that of bulk TiO_2. Since rutile (1 1 0) surface is thermodynamically stable, it has been extensively investigated. The filled valence band is composed of O 2p orbitales and the empty conduction band is composed of Ti 3d, 4s, and 4p orbitals. The Ti 3d orbitals dominate the lower portion of the conduction band. Studies have shown that anatase TiO_2 (1 0 1) exhibits the similar photoemission behaviour to that of rutile [81].

Asahi et al. [14] had proven that non-metal ion doping would change the crystal structure and the band structure of TiO_2. Generally the doped impurities in the modified TiO_2 are located at different sites, for substitution of Ti, O, interstitial, chemisorption, and physisorption sites, depending on the chemical nature of dopants.

4.2. Effects of F doping

The band structure of fluorine doped TiO_2, observed from UV-vis, suggests its significant difference from other non-metal element doped TiO_2 photocatalysts. Most studies in F-doping showed that F-doping could not change the absorption property of TiO_2, neither in band gap narrowing nor in production of new absorption bands, as shown in Fig. 1(B) [45,46,53,59–61]. As mentioned above, the experimental results were in accordance well with the theoretical analysis [14,61]. According to the mechanism of band-gap photoexcitation [81], F doped TiO_2 could not induce photocatalytic reactions under visible light irradiation. Actually, the early studies of fluorine modification targeted at improving the UV activity of TiO_2 [28–31]. However, it was surprising that the visible photocatalytic activity of F doped TiO_2 has been reported by many groups

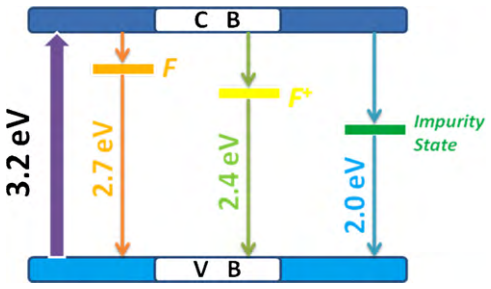

Scheme 1. Schematic band gap structure of F-doped TiO_2 [59,60].

recently [53,55,59,60,82] and two mechanisms have been proposed to account for the phenomenon.

Li et al. [59,60] suggested that the photocatalytic activity of F doped TiO_2 at visible light would be attributed to oxygen vacancies. Two kinds of oxygen vacancies (F and F^+ centres) were found in the F-doped TiO_2 by photoluminescence (PL) spectra. These vacancies led to two energy levels below the CB at 0.53 and 0.84 eV, respectively. Moreover, an impurity energy state below the CB of TiO_2 was also observed. Therefore the band gap structure could be schematically shown in Scheme 1 [59,60]. Emeline et al. [83–85] reported the defect-induced red-shift of a wide band gap on metal oxide solids, i.e. TiO_2, ZnO, MgO, and BeO, although the origin of the defects was UV pre-irradiation. In addition, Nakamura et al. [86] suggested the O vacancies were also responsible for the photocatalytic activity under visible light irradiation.

Another possible origin for visible response of F-doped TiO_2 could be attributed to the formation of Ti^{3+} which had been observed in the fluorine modified TiO_2 by many groups [24,35,44,53]. Two types of doping F, insertion in the bulk (Ti-F-Ti) and adsorption on the surface (Ti-F), were found by Yu et al. [24] and Czoska et al. [44]. In the former case, F^- doped into O^{2-} site requires one extra electron for charge compensation, inducing the formation of Ti^{3+}. In the surface F^- adsorption, an isoelectronic OH^- would compensate the charge imbalance from F^- substitution of O^{2-}. In both cases, O vacancies are not necessary for the insertion of fluorine in TiO_2 matrix. Yu et al. [24,53] suggested that Ti^{3+} could only enhance the UV activity of TiO_2 and the visible response was attributed to O vacancies. Czoska et al. [44] found that Ti^{3+} could be formed without generating O vacancies and concluded that both Ti^{3+} and surface fluorine were responsible for the visible response of F-doped TiO_2. DFT calculations showed that Ti^{3+} induced a defect state at 0.6 eV below the conduction band. This state is of higher energy than that of Ti^{3+} states associated with O vacancies.

Therefore, F-doping produced two types of species, oxygen vacancy and Ti^{3+}. These species have low energy barrier in response to visible light and can activate organic molecules or oxygen to induce redox reaction. Previous investigations indicated that the oxygen vacancies and Ti^{3+} in TiO_2 would result in significant changes of UV-vis absorption [83–86]. However, for F-doped TiO_2, no such changes were observed from the spectra (Fig. 1(B)). The possible suggestion would be the weak intensity and the balance between blue-shift and red-shift from oxygen vacancies and Ti^{3+}. Further studies would be directed to elucidate the role of F-doping in visible response.

4.3. Effects of Cl or Br doping

Different from fluorine doped TiO_2, UV-vis of chlorine doped TiO_2 showed narrower band gap and new absorption bands in visible light region [56,63,87], which is similar to N-doping, as shown in Fig. 1(C). Further studies suggested that Cl-doped TiO_2 is able to photocatalytically degrade organic pollutants under visible light. The mechanism of the visible light response for chlorine doped TiO_2 has not been proposed so far. Li et al. [63] found that the anatase and rutile crystallites in the plasma generated TiO_2 powders had an approximate chemical composition of $TiO_{1.98}Cl_x$, which suggested the presence of oxygen vacancies due to chlorine doping. The Cl doping at chemical state of −1 might follow the similar visible response mechanism as the O vacancies in F doped TiO_2.

For Br doping, no single Br doped TiO_2 has ever been synthesised. The studies on Br doping have always been in co-doping with other elements, such as Cl [52], N [55], and Sm [47]. It is imprudent to discuss the effect of Br doping on the crystal and band structure as well as visible response mechanism of TiO_2 without taking into account the synergistic effect of other doping ions. However, all the studies of co-doping clearly showed that Br doping would significantly improve the optical absorption to lower band gap energy than single Cl, N, or Sm doping [47,52,55]. Gao et al. [47] proposed that Br would bind to Ti and form Ti-Br bond producing a new defect band between CB and VB, consequently increasing the response to visible light.

4.4. Effects of I modification

Long et al. [88] employed DFT calculations to analyse the electronic structure of I-doped TiO_2 with I^{5+} substitution of Ti^{4+} and found that I 5p orbitals would mix with O 2p and Ti 3d orbitals and contribute to VB and CB, respectively. Moreover, the band potentials would shift downwards and have a stronger oxidation potential [88]. Tojo et al. [33] used time-resolved diffuse reflectance (TDR) to study the transient behaviour of the photogenerated charge carriers of I-doped TiO_2 under UV and visible irradiations. Based on the results, they proposed that the continuous states consisting of 5p and/or 5s orbitals of I^{5+} and O 2p orbitals of the valence band are favourable for efficient trapping of h^+ at the I-induced states, as shown in Scheme 2 [33].

DFT calculations was also applied by Long et al. [89] to investigate the structural and electronic properties of iodine doped anatase and rutile TiO_2. They suggested that I 5p states mixing with Ti 3d and O 2p states resulted in a move to higher energy region and induced band gap narrowing, while the substitution of I to O, a blue-shift would occur. For I-doped rutile TiO_2, the red-shift was similar to anatase system but an indirect band gap reduced efficiency and the nature of the red-shift was ascribed to I 5p states.

Different from HIO_3, KIO_3 could lead to multivalency (I^{7+}/I^-) iodine doped TiO_2 via a hydrothermal process [54]. I^{7+} can be presented in the form of periodate (IO_4^-) and the ionic radius of I^- (0.216 nm) is much larger than that of O^{2-} (0.124 nm) or Ti^{4+} (0.068 nm), thus the substitution of O^{2-} or Ti^{4+} would hardly occur. Su et al. [65] suggested that the I^{7+}/I^- species were dispersed on the surface of anatase particles rather than the substitution. With the DFT calculations, they proposed a sub-band-band mechanism for the visible light photoactivity on the multivalency I doped TiO_2 [65]. The redox potential $E^0(I^{7+}/I^-) = 1.24$ V lies between the conduction band $E_{cb}(TiO_2) = -0.5$ V and the valence band $E_{vb}(TiO_2) = 2.7$ V (versus NHE); therefore the excitation of an electron from the valence band of TiO_2 to the surface I species is feasible. Theoretical results also revealed that the new states originated from the I atoms of IO_4^- group near the bottom of conduction band and suggested a possible electron excitation from the valence band of TiO_2 to the surface IO_4^-. The holes left on the valence band of TiO_2 could oxidise hydroxyl to hydroxyl radicals ($OH^\bullet$). The detailed illustration is shown in Scheme 3 [65].

A novel type of iodine modification of TiO_2 with $(I_2)_n$ encapsulation inside TiO_2 was also discovered [48]. In the investigation, I_2 was used as a dye, due to (i) its high solubility in titanium isopropoxide, (ii) the relative lower boiling point (about 184 °C), and the reducing environment providing by Ti–OR can prevent I_2 fur-

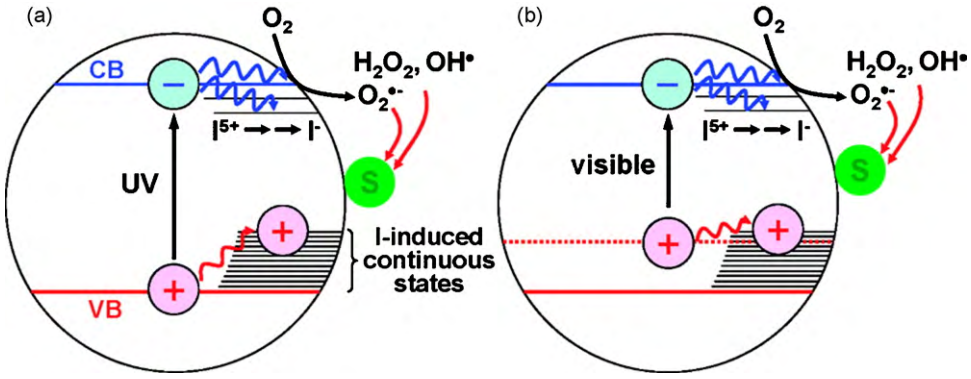

Scheme 2. Schematic illustration of the I-TiO_2 photocatalytic reaction processes under UV- (a) and visible-light (b) irradiation. [33].

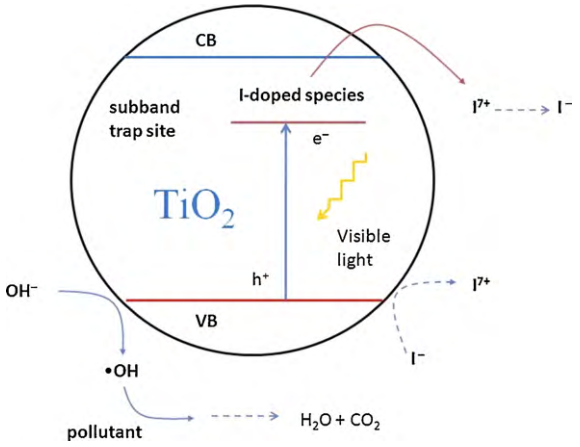

Scheme 3. Proposed photocatalytic mechanisms over I-doped TiO_2 [65].

ther oxidation. UV-vis spectra of the iodine modified TiO_2 showed a broad absorption band at 400–667 nm. The visible response possibly follows a dye-sensitised mechanism. The dye $(I_2)_n$ absorbing a visible photon is promoted into an excited electronic state $(I_2)_n^*$, from which an electron can be transferred into the conduction band of the semiconductor as follows.

$$(I_2)_n + h\nu \rightarrow (I_2)_n^* \quad (4)$$

$$(I_2)_n^* + TiO_2 \rightarrow [(I_2)_n]^+ + TiO_2(e^-) \quad (5)$$

Once the electron is injected into the conduction band and transferred to the photocatalyst surface, the photocatalytic reaction under visible light irradiation occurs [48].

5. Photocatalytic activity

Many heterogeneous photocatalytic reactions have been carried out to evaluate the activity of halogen modified TiO_2 photocatalysts. For aqueous phase reactions, various organic chemicals, e.g., 4-chlorophenol, phenol, methylene blue, methyl orange, rhodamine B and oxalic acid, have been used as model pollutants. For gaseous photocatalytic reactions, acetone, acetaldehyde, formaldehyde, and trichloroethylene have been widely tested. In those photocatalytic reactions, many experimental parameters were involved, such as organic pollutant, initial concentration, surface area and amount of catalyst, temperature, and light source (irradiation spectra). Thus, a comparison of the photocatalytic activities from laboratory to laboratory is much challenging even though Degussa P25 was generally used as a reference [90].

Fig. 2 shows the typical experimental results of photooxidation of aqueous phenol and gaseous acetone using iodine doped TiO_2 [38,65]. The photooxidation of phenol was carried out using a 1000-W Xe lamp and visible-light-activated photocatalytic activity was tested with the irradiation above 400 nm using a cut-off filter. The distance between the light source and surface of solution was 100 cm, and the temperature of phenol solution was about 25 °C. The concentration of phenol was monitored by a colorimeter [38]. Fig. 2(A) shows that, compared to pure TiO_2 and P25, I-TiO_2 could efficiently decompose phenol under visible light irradiation. On the other hand, photodegradation of gaseous acetone was done in a 2500 mL glass container, which was connected to a quartz reactor with an inner size of 15 mm × 15 mm × 2 mm and interfaced to a gas chromatograph. A closed circulation reaction system, including the container, the reactor, and the GC, was established with the aid of

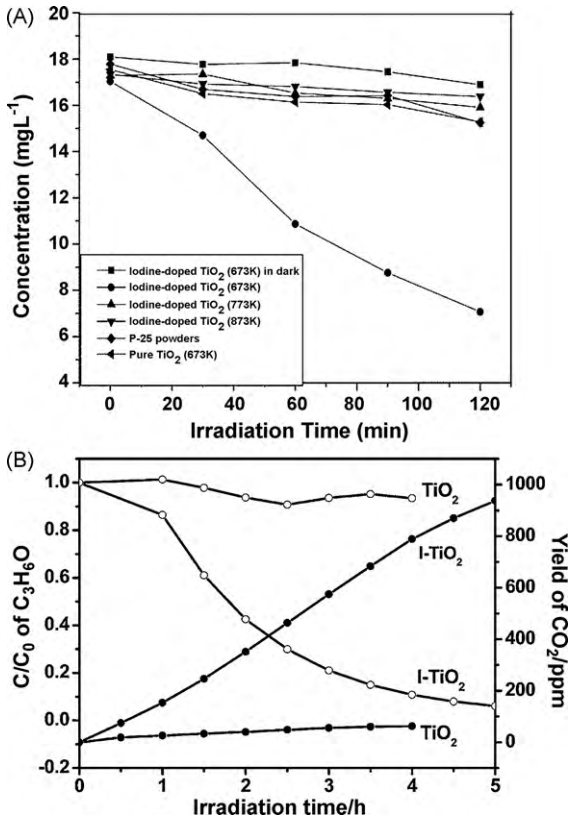

Fig. 2. Comparison of photocatalytic activity of pure and I-modified TiO_2, (A) Photodegradation of phenol solutions in the presence of I-doped TiO_2, P25 powders, and pure TiO_2 nanoparticles (673 K) under visible light irradiation (λ > 400 nm) and absorption of phenol on I-doped TiO_2 (673 K) in dark; [38] (B) Photooxidation of gaseous acetone over I-TiO_2 and TiO_2 under visible light irradiation. The symbols ○ and ● represent C_3H_6O and CO_2, respectively. [65].

Table 3
Preparation, property and activity (degradation of dyes) of halogen modified TiO_2 photocatalysts.

Synthesis	Precursor	Calcination	Crystalline[a]	Dopant/level[b]	Band gap[c] (eV)	Chemical	Light (nm)/time (min)	Activity/reference: activity	Ref.
Ion implantation	F^+	1200 °C/5 h	R	F^-/0.43 mol%	/	/	/	/	[61]
Pyrolysis	$(NH_4)_2TiF_6$	600 °C/1 h	A	F/13.4 mol% N/1.7 mol%	3.05	Methylene blue	>420/390	40%/P25: 20%	[91]
Sol–gel	NH_4F and CF_3COOH	600 °C/1 h	A, R	F/16 mol%	~ 3.10	/	/	/	[46]
Sol–gel	HF	500 °C/1 h	A	F/-	3.20	/	/	/	[44]
Sol–gel	NH_4F	100 °C/4 h	A	F/2.72 mol% N/2.18 mol%	2.44	Methyl orange	>420/360	95%/P25: 30%	[43]
Sol–gel	BF_3•$2CH_3CO_2$	80 °C/18 h	A	F/3.3 mol% B/low	3.10	Methylene blue	>420/180	60%/P25: 35%	[42]
CVD	NH_4F	600 °C/2 h	A, R	F/-	~3.20	Methyl orange	>400/180	70.5%/undoped TiO_2: 12.1%	[95]
				B/-					
Hydrothermal	$TiCl_4$	150 °C/12 h	R	Cl/0.7 mol%	2.99	Rhodamine B	>420/240	85%/P25: 15%	[56]
Ratio frequency thermal plasma	$TiCl_3$	/	A, R	Cl	2.65	Methyl orange	405/120	95%/P25: 60%	[63]
Hydrothermal	cetyltrimethylammonia bromide	100 °C/5 h	A, B	Br/-	1.88	Methylene blue	UV/80	85%/P25: 95%	[55]
				N/-			>420/960	50%/P25: 18%	
Sol–gel	NH_4Br	700 °C/2 h	A, R	Br/1 mol% Sm/0.75 mol%	3.10	/	/	/	[47]
Hydrothermal	HIO_3	400 °C/2 h	A, R	I^{5+}/5.2 mol%	~ 2.48	Methylene blue	UV-vis/240 >420/240	90%/P25: 40% 90%/P25: 20%	[54]
Hydrothermal	HIO_4	400 °C/2 h	A	I^{7+}/8.9 mol%	3.14	Rhodamine B	UV-vis/12 >420/90	99%/P25: 60% 99%/P25: 20%	[57]
Sol–gel	I_2	300 °C/6 h	A, R	I_2/–	~ 3.10	Methylene blue	Sunlight/2 d	10 times/P25	[48]

[a] A means anatase, B means brookite, and R means rutile crystalline phase.
[b] Dash is used if there are no data available.
[c] The results represent the intrinsic band gap energies.

Table 4
Preparation, property and activity (photodegradation of non-absorbing-visible organics) of halogen modified TiO_2 photocatalysts.

Synthesis	Precursor	Calcination	Crystal[a]	Dopant/level[b]	Band gap[c] (eV)	Chemical	Light (nm)/time (min)	Activity/reference: activity	Ref.
Hydrothermal	TiF_4	180 °C/12 h	A	F^-/2.2 to 4.6 mol%	~3.10	4-chlorophenol	>400/360	50%/without photocatalyst: 0	[53]
Sol–gel-solvothermal	NH_4F	140 °C/10 h	A, R	F/- N/-	3.20	4-chlorophenol	350–400/720 400–500/720	43.1%/P25: 26.6% 17.8%/P25: 10.2%	[64]
Electrochemical anodization	HF	/	A	F/0.54 mol% S/0.93 mol%	~3.20	4-chlorophonol	>400/180	85.8%/F-TiO_2: 46.1%	[62]
Calcination-hydrothermal	HCl	500 °C/3 h	A	Cl/- N/-	2.88	phenol	>390/120	13/TiO_2: 3 (Rate: 10^{-7} mol l^{-1} min^{-1})	[96]
Hydrolysis	HCl	300 °C/2 h	A, R	Cl/-	~3.00	phenol	>400/120	42.5%/P25: 12.0%	[87]
Hydrolysis	HIO_3	400 °C	A, B, R	I^{5+}/-	2.81	phenol	>400/120	41.2%/P25: 5.9%	[38]
Hydrothermal	HIO_3	400 °C/3 h	A, B	I^{5+}/4 mol%	1.40–2.20	4-chlorophenol	>440/360	60%/ST-01: 0	[33]
Hydrolysis	HIO_3	400 °C/2 h	A, R	I^{5+}/14.3 mol% La^{3+}/14.3 mol%	2.64	oxalic acid	>400/120	98%/I-TiO_2: 25%	[39]
Hydrolysis	HIO_3	400 °C	A	I^-, I^{5+}, I^{7+}/- Ce^{3+}, Ce^{4+}/-	1.71	oxalic acid	>400/180	90%/I-TiO_2: 37%	[40]

[a] A means anatase, B means brookite, and R means rutile crystalline phase.
[b] Dash is used if there are no data available.
[c] The results represent the intrinsic band gap energies.

a circulation pump. The quartz reactor was irradiated with a 500 W tungsten halogen lamp positioned inside a cylindrical Pyrex vessel and surrounded by a circulating water jacket to cool the lamp. A cut-off filter was placed outside the Pyrex jacket to completely remove all wavelengths less than 420 nm to ensure irradiation with visible light [65]. Fig. 2(B) reveals that I-TiO_2 could decompose acetone under visible light and that the catalytic activity was much better than pure TiO_2.

Here we summarise the photocatalytic activities of halogen doped TiO_2 according to the type of pollutants as aqueous dyes (Table 3), aqueous non-absorbing-visible organics (Table 4), and gaseous organics (Table 5).

Table 3 presents the activities of various halogen modified TiO_2 in photodegradation of dyes, such as methyl blue, methyl orange, and rhodamine B. Under visible light irradiation ($\lambda > 420$ nm), chlorine-doped rutile TiO_2 showed the highest activity, with an enhancement factor of 5.83 over P25 [56]. Iodine-doped TiO_2 showed inferior activities with the enhancement factor of 4.95 [57] and fluorine-doped TiO_2 exhibited the lowest activities [42,91]. For the organics without absorbing visible light, such as phenol and 4-chlorophenol, the activities of photocatalysts were generally evaluated under irradiation above 400 nm, as shown in Table 4. Compared to P25, iodine-doped TiO_2 showed the highest activity, and the enhancement factor was 6.98 [38], while fluorine-doped TiO_2 enhanced the activity less than 2 times [62,64]. It is noted that codoping generally produced higher activity than that of single element doping. For instance, the activity of F-S-codoped TiO_2 was 1.86 times as high as that of F-doped TiO_2. Also, La or Ce codoped with I was more efficient than single I doping by an enhancement factor of 3.92 and 2.43, respectively. Surprisingly, fluorine-doped TiO_2 showed higher activity in gaseous phase photocatalytic reactions, as shown in Table 5, and achieved the enhancement over P25 by 4.55 times high in the photodegradation of gaseous acetaldehyde [60]. From the above available data, we can conclude that halogen modified TiO_2 shows varying performance in different reaction systems. The detailed mechanism has not been elucidated. Two possible reasons have to be taken into account. For dye degradation in aqueous solution, dye molecules actually can absorb visible light, and sometimes their visible absorption is stronger than that of modified TiO_2, which makes it difficult to identify the activity contributed from the catalyst. For aqueous phase reaction, the surface of a photocatalyst is dominantly covered by water molecules. Then, plenty of hydroxyls are provided, and surface defects of oxygen vacancies or Ti^{3+} are partially compensated by dissociative water from adsorption [92], leading to inferior influence of surface characteristics on photoactivity in liquid phase.

Before being committed to practical application, the stability and safety of halogen modified TiO_2 need to be comprehensively investigated, as what has been done to pure TiO_2 [93]. Long et al. [89] theoretically proved that iodine doped TiO_2 has a much more efficient and stable photocatalytic performance than the pristine TiO_2. Padmanabhan et al. [94] reported that fluorine doping would maintain anatase phase stable up to a temperature as high as 900 °C. Luo et al. [52] investigated the stability of Br-Cl codoped TiO_2 in photocatalytic reactions in three runs of regeneration, and they found that the evolution rates of H_2 and O_2 were constant in each run. However, the photocatalytic performance of long-term use and lifetime of the modified TiO_2 still lack of sufficient data, which needs further investigation. Also, the safety of halogen modified TiO_2 has not been explored yet. Generally, halogen element is bonded to TiO_2 matrix at relative low doping levels but with high chemical and thermal stability and, thus the catalysts would be safe to human and the environment as pure TiO_2.

The results in Tables 3–5 for photocatalytic reactions using halogen element modified TiO_2 demonstrate that halogen modified TiO_2 exhibited high efficiency of photocatalysis for a wide range of

Table 5
Preparation, property and activity (photodegradation of gaseous organics or water) of halogen modified TiO_2 photocatalysts.

Synthesis	Precursor	Calcination	Crystal[a]	Dopant/level[b]	Band gap[c] (eV)	Chemical	Light (nm)/time (min)	Activity/reference: activity	Ref.
Spray pyrolysis	H_2TiF_6	900 °C	A	F^-/1.8–9.5 mol%	3.2	Acetaldehyde Trichloroethylene	>420/360	1000/P25: 220 690/P25: 180 (CO_2 evolution: ppm)	[60]
Spray pyrolysis	H_2TiF_6	900 °C	A	F^-/1.8–9.5 mol%	3.24	Acetaldehyde	UV/120	1290/P25: 1190 (CO_2 evolution: ppm)	[59]
Sol–gel	NH_4F and CF_3COOH	400 °C/1 h	A, R	F/16 mol%	~3.10	Acetone	UV/60	700/P25: 350 (CO_2 evolution: ppm	[45]
Hydrothermal	HBr	100 °C/1 d	A, B, R	Br/0.5–1.8 mol% Cl/0.6–2.7 mol%	2.85	H_2O	UV/480	1200/P25: 500 (H_2 evolution: μmol)	[52]
Deposition-precipitation-hydrothermal	KIO_3	300 °C/2 h	A	I^-, I^{7+}	~3.1	Acetone	>420/240	94%/P25: 0 (acetone degradation)	[65]

[a] A means anatase, B means brookite, and R means rutile crystalline phase.
[b] Dash is used if there are no data available.
[c] The results represent the intrinsic band gap energies.

organics in aqueous or gaseous phases with visible region. The photocatalytic performance, at some extent, depends on certain target pollutions. For instance, chlorine doped TiO_2 prefers to degrade dyes, iodine doped TiO_2 shows superior activity for organics without the ability of responding visible, and fluorine doped TiO_2 is more suitable for gas phase reaction. The detailed mechanism and relationship between doping types with target pollutants still need further elucidation.

6. Summary and perspective

Halogen elements provide both cation and anion to substitute Ti^{4+} and/or O^{2-} in TiO_2 matrix, which has attracted much attentions in the development of halogen modified TiO_2 for visible light photocatalysis. Various synthesis routes, such as hydrolysis, precipitation, pyrolysis, sol–gel and hydrothermal synthesis, have been applied to prepare the visible-light-induced TiO_2-based photocatalysts. The precursor of the doping ion will greatly influence the chemical states of the impurities of the doped samples. Fluorine, chlorine and bromine generally exist in the TiO_2 matrix with a chemical state of −1, indicating their substitutions of O^{2-} in TiO_2 crystal; however, iodine usually is present as cation (+5 and +7) for occupying the Ti sites. The surface properties of TiO_2 could be significantly improved by halogen doping, such as the enhancement of surface acidity, formation of the surface hydroxyl radicals, creation of active site and oxygen vacancies or Ti^{3+}. The optical properties are in general controlled by the chemical nature of dopants, which may partially reflect the band structures of the modified TiO_2. The experiments and DFT computations have revealed that different kinds of ion or chemical state contribute to the changes of the band structure. Fluorine-doping usually does not change the optical feature of TiO_2, while iodine-doping can dramatically narrow the band gap of TiO_2 to 1.40 eV. Compared to undoped TiO_2, most of the doped samples showed higher efficiencies for photocatalytic oxidation of gaseous/aqueous pollutants under both UV and visible light irradiations.

Compared to the studies on nitrogen doped TiO_2, further extensive attention needs to be paid on the topic of halogen modification. The simple and efficient synthesis, which is able to control the crystal phase, surface feature, and band structure (not only the band gap, but also the position of CB and VB) thereafter improving the efficiency under both UV and visible light, is still to be developed. The mechanism of visible light response from halogen doping requires more efforts to investigate, from experimental using novel characterisations to computational techniques, are strongly recommended.

Acknowledgement

We gratefully acknowledge Australian government, Cooperative Research Centre for Contamination Assessment and Remediation of Environment (CRC-CARE), for supporting the project.

References

[1] M.R. Hoffmann, S.T. Martin, W.Y. Choi, D.W. Bahnemann, Chem. Rev. 95 (1995) 69–96.
[2] X. Chen, S.S. Mao, Chem. Rev. 107 (2007) 2891–2959.
[3] H.Q. Sun, Y. Bai, Y.P. Cheng, W.Q. Jin, N.P. Xu, Indust. Eng. Chem. Res. 45 (2006) 4971–4976.
[4] L.L. Tinker, N.D. McDaniel, S. Bernhard, J. Mater. Chem. 19 (2009) 3328–3337.
[5] Y.H. Zhang, S.G. Ebbinghaus, A. Weidenkaff, T. Kurz, H.A.K. von Nidda, P.J. Klar, M. Gungerich, A. Reller, Chem. Mater. 15 (2003) 4028–4033.
[6] S. Yuan, Q.R. Sheng, J.L. Zhang, H. Yamashita, D.N. He, Microporous Mesoporous Mater. 110 (2008) 501–507.
[7] X.S. Li, G.E. Fryxell, C. Wang, M.H. Engelhard, Microporous Mesoporous Mater. 111 (2008) 639–642.
[8] T. Hirai, K. Suzuki, I. Komasawa, J. Colloid Interf. Sci. 244 (2001) 262–265.

[9] Y. Bessekhouad, D. Robert, J.V. Weber, Catal. Today 101 (2005) 315–321.
[10] R. Brahimi, Y. Bessekhouad, A. Bouguelia, M. Trari, J. Photochem. Photobiol. A-Chem. 194 (2008) 173–180.
[11] D. Duonghong, E. Borgarello, M. Gratzel, J. Am. Chem. Soc. 103 (1981) 4685–4690.
[12] E. Borgarello, J. Kiwi, E. Pelizzetti, M. Visca, M. Gratzel, J. Am. Chem. Soc. 103 (1981) 6324–6329.
[13] G.K. Mor, K. Shankar, M. Paulose, O.K. Varghese, C.A. Grimes, Nano Lett. 6 (2006) 215–218.
[14] R. Asahi, T. Morikawa, T. Ohwaki, K. Aoki, Y. Taga, Science 293 (2001) 269–271.
[15] S.U.M. Khan, M. Al-Shahry, W.B. Ingler, Science 297 (2002) 2243–2245.
[16] H.Q. Sun, Y. Bai, W.Q. Jin, N.P. Xu, Solar Energy Mater. Solar Cells 92 (2008) 76–83.
[17] H.Q. Sun, Y. Bai, H.J. Liu, W.Q. Jin, N.P. Xu, J. Photochem. Photobiol. A-Chem. 201 (2009) 15–22.
[18] H.Q. Sun, Y. Bai, H.J. Liu, W.Q. Jin, N.P. Xu, G.J. Chen, B.Q. Xu, J. Phys. Chem. C 112 (2008) 13304–13309.
[19] S. Sakthivel, H. Kisch, Angew. Chem. Int. Ed. 42 (2003) 4908–4911.
[20] Y.P. Cheng, H.Q. Sun, W.Q. Jin, N.P. Xu, Chem. Eng. J. 128 (2007) 127–133.
[21] Y.P. Cheng, H.Q. Sun, W.Q. Jin, N.P. Xu, Chin. J. Chem. Eng. 15 (2007) 178–183.
[22] J.C. Yu, W.K. Ho, J.G. Yu, H. Yip, P.K. Wong, J.C. Zhao, Environ. Sci. Technol. 39 (2005) 1175–1179.
[23] Q. Shi, D. Yang, Z.Y. Jiang, J. Li, J. Mol. Catal. B-Enzym. 43 (2006) 44–48.
[24] J.C. Yu, J.G. Yu, W.K. Ho, Z.T. Jiang, L.Z. Zhang, Chem. Mater. 14 (2002) 3808–3816.
[25] H.M. Yates, M.G. Nolan, D.W. Sheel, M.E. Pemble, J. Photochem. Photobiol. A-Chem. 179 (2006) 213–223.
[26] C. Di Valentin, E. Finazzi, G. Pacchioni, A. Selloni, S. Livraghi, M.C. Paganini, E. Giamello, Chem. Phys. 339 (2007) 44–56.
[27] X.F. Qiu, C. Burda, Chem. Phys. 339 (2007) 1–10.
[28] A. Hattori, K. Shimoda, H. Tada, S. Ito, Langmuir 15 (1999) 5422–5425.
[29] C. Minero, G. Mariella, V. Maurino, E. Pelizzetti, Langmuir 16 (2000) 2632–2641.
[30] A. Hattori, H. Tada, J. Sol–Gel Sci. Technol. 22 (2001) 47–52.
[31] M.S. Vohra, S. Kim, W. Choi, J. Photochem. Photobiol. A-Chem. 160 (2003) 55–60.
[32] R.C. Weast, CRC Handbook of Chemistry and Physics. 70th eds. Boca Raton, Frorida, 1989.
[33] S. Tojo, T. Tachikawa, M. Fujitsuka, T. Majima, J. Phys. Chem. C 112 (2008) 14948–14954.
[34] Q. Wang, C.C. Chen, W.H. Ma, H.Y. Zhu, J.C. Zhao, Chem.-A Eur. J. 15 (2009) 4765–4769.
[35] K.S. Yang, Y. Dai, B.B. Huang, M.H. Whangbo, Chem. Mater. 20 (2008) 6528–6534.
[36] Q.H. Zhang, L. Gao, J.K. Guo, Appl. Catal. B-Environ. 26 (2000) 207–215.
[37] Q.H. Zhang, L. Gao, J.K. Guo, J. Eur. Ceram. Soc. 20 (2000) 2153–2158.
[38] X.T. Hong, Z.P. Wang, W.M. Cai, F. Lu, J. Zhang, Y.Z. Yang, N. Ma, Y.J. Liu, Chem. Mater. 17 (2005) 1548–1552.
[39] Z.Q. He, X. Xu, S. Song, L. Xie, J.J. Tu, J.M. Chen, B. Yan, J. Phys. Chem. C 112 (2008) 16431–16437.
[40] S. Song, J.J. Tu, L.J. Xu, X. Xu, Z.Q. He, J.P. Qiu, J.G. Ni, J.M. Chen, Chemosphere 73 (2008) 1401–1406.
[41] C. Su, B.Y. Hong, C.M. Tseng, Catal. Today 96 (2004) 119–126.
[42] E.A. Reyes-Garcia, Y.P. Sun, D. Raftery, J. Phys. Chem. C 111 (2007) 17146–17154.
[43] Y. Xie, Y.Z. Li, X.J. Zhao, J. Mol. Catal. A-Chem. 277 (2007) 119–126.
[44] A.M. Czoska, S. Livraghi, M. Chiesa, E. Giamello, S. Agnoli, G. Granozzi, E. Finazzi, C. Di Valentin, G. Pacchioni, J. Phys. Chem. C 112 (2008) 8951–8956.
[45] N. Todorova, T. Giannakopoulou, G. Romanos, T. Vaimakis, J.G. Yu, C. Trapalis, Int. J. Photoenergy (2008). Article ID 721824.
[46] N. Todorova, T. Giannakopoulou, T. Vaimakis, C. Trapalis, Mater. Sci. Eng. B-Adv. Funct. Solid-State Mater. 152 (2008) 50–54.
[47] C.M. Gao, H.W. Song, L.Y. Hu, G.H. Pan, R.F. Qin, F. Wang, Q.L. Dai, L.B. Fan, L.N. Liu, H.H. Liu, J. Lumin. 128 (2008) 559–564.
[48] S. Usseglio, A. Damin, D. Scarano, S. Bordiga, A. Zecchina, C. Lamberti, J. Am. Chem. Soc. 129 (2007) 2822–2828.
[49] A. Testino, I.R. Bellobono, V. Buscaglia, C. Canevali, M. D'Arienzo, S. Polizzi, R. Scotti, F. Morazzoni, J. Am. Chem. Soc. 129 (2007) 3564–3575.
[50] H.S. Hafez, Mater. Lett. 63 (2009) 1471–1474.
[51] N. Murakami, Y. Kurihara, T. Tsubota, T. Ohno, J. Phys. Chem. C 113 (2009) 3062–3069.
[52] H.M. Luo, T. Takata, Y.G. Lee, J.F. Zhao, K. Domen, Y.S. Yan, Chem. Mater. 16 (2004) 846–849.
[53] W. Ho, J.C. Yu, S. Lee, Chem. Commun. (2006) 1115–1117.
[54] G. Liu, Z.G. Chen, C.L. Dong, Y.N. Zhao, F. Li, G.Q. Lu, H.M. Cheng, J. Phys. Chem. B 110 (2006) 20823–20828.
[55] Y.G. Sheng, Y. Xu, D. Jiang, L.P. Liang, D. Wu, Y.H. Sun, Int. J. Photoenergy (2008).
[56] H. Xu, Z. Zheng, L.Z. Zhang, H.L. Zhang, F. Deng, J. Solid State Chem. 181 (2008) 2516–2522.
[57] G. Liu, C.H. Sun, X.X. Yan, L. Cheng, Z.G. Chen, X.W. Wang, L.Z. Wang, S.C. Smith, G.Q. Lu, H.M. Cheng, J. Mater. Chem. 19 (2009) 2822–2829.
[58] K.Y. Jung, S.B. Park, H.D. Jang, Catal. Commun. 5 (2004) 491–497.
[59] D. Li, H. Haneda, S. Hishita, N. Ohashi, N.K. Labhsetwar, J. Fluorine Chem. 126 (2005) 69–77.
[60] D. Li, H. Haneda, N.K. Labhsetwar, S. Hishita, N. Ohashi, Chem. Phys. Lett. 401 (2005) 579–584.
[61] T. Yamaki, T. Umebayashi, T. Sumita, S. Yamamoto, M. Maekawa, A. Kawasuso, H. Itoh, Nucl. Instrum. Methods Phys. Res. Sec. B-Beam Int. Mater. Atoms 206 (2003) 254–258.
[62] X.Q. Chen, Y.L. Su, X.W. Zhang, L.C. Lei, Chin. Sci. Bull. 53 (2008) 1983–1987.
[63] J.G. Li, M. Ikeda, C.C. Tang, Y. Moriyoshi, H. Hamanaka, T. Ishigaki, J. Phys. Chem. C 111 (2007) 18018–18024.
[64] D.G. Huang, S.J. Liao, J.M. Liu, Z. Dang, L. Petrik, J. Photochem. Photobiol. A-Chem. 184 (2006) 282–288.
[65] W.Y. Su, Y.F. Zhang, Z.H. Li, L. Wu, X.X. Wang, J.Q. Li, X.Z. Fu, Langmuir 24 (2008) 3422–3428.
[66] E.M. Rockafellow, L.K. Stewart, W.S. Jenks, Appl. Catal. B-Environ. 91 (2009) 554–562.
[67] Y.M. Chen, F. Chen, J.L. Zhang, Appl. Surf. Sci. 255 (2009) 6290–6296.
[68] J.W. Tang, H.D. Quan, J.H. Ye, Chem. Mater. 19 (2007) 116–122.
[69] Y. Yu, H.H. Wu, B.L. Zhu, S.R. Wang, W.P. Huang, S.H. Wu, S.M. Zhang, Catal. Lett. 121 (2008) 165–171.
[70] K. Suriye, P. Praserthdam, B. Jongsomjit, Appl. Surf. Sci. 253 (2007) 3849–3855.
[71] H. Irie, Y. Watanabe, K. Hashimoto, J. Phys. Chem. B 107 (2003) 5483–5486.
[72] J. Wang, D.N. Tafen, J.P. Lewis, Z.L. Hong, A. Manivannan, M.J. Zhi, M. Li, N.Q. Wu, J. Am. Chem. Soc. 131 (2009) 12290–12297.
[73] S. Ikeda, N. Sugiyama, S. Murakami, H. Kominami, Y. Kera, H. Noguchi, K. Uosaki, T. Torimoto, B. Ohtani, Phys. Chem. Chem. Phys. 5 (2003) 778–783.
[74] S. Takeda, S. Suzuki, H. Odaka, H. Hosono, Thin Solid Films 392 (2001) 338–344.
[75] R. Scotti, I.R. Bellobono, C. Canevali, C. Cannas, M. Catti, M. D'Arienzo, A. Musinu, S. Polizzi, M. Sommariva, A. Testino, F. Morazzoni, Chem. Mater. 20 (2008) 4051–4061.
[76] I. Sopyan, M. Watanabe, S. Murasawa, K. Hashimoto, A. Fujishima, Chem. Lett. (1996) 69–70.
[77] A.A. Levchenko, G.S. Li, J. Boerio-Goates, B.F. Woodfield, A. Navrotsky, Chem. Mater. 18 (2006) 6324–6332.
[78] M.M. Ren, R. Ravikrishna, K.T. Valsaraj, Environ. Sci. Technol. 40 (2006) 7029–7033.
[79] D.C. Hurum, A.G. Agrios, K.A. Gray, T. Rajh, M.C. Thurnauer, J. Phys. Chem. B 107 (2003) 4545–4549.
[80] G.H. Li, K.A. Gray, Chem. Mater. 19 (2007) 1143–1146.
[81] A.L. Linsebigler, G.Q. Lu, J.T. Yates, Chem. Rev. 95 (1995) 735–758.
[82] D.G. Huang, S.J. Liao, S.Q. Quan, L. Liu, Z.J. He, J.B. Wan, W.B. Zhou, J. Mater. Sci. 42 (2007) 8193–8202.
[83] A.V. Emeline, G.V. Kataeva, V.K. Ryabchuk, N. Serpone, J. Phys. Chem. B 103 (1999) 9190–9199.
[84] A.V. Emeline, G.N. Kuzmin, D. Purevdorj, V.K. Ryabchuk, N. Serpone, J. Phys. Chem. B 104 (2000) 2989–2999.
[85] A.V. Emeline, G.V. Kataeva, A.V. Panasuk, V.K. Ryabchuk, N.V. Sheremetyeva, N. Serpone, J. Phys. Chem. B 109 (2005) 5175–5185.
[86] I. Nakamura, N. Negishi, S. Kutsuna, T. Ihara, S. Sugihara, E. Takeuchi, J. Mol. Catal. A-Chem. 161 (2000) 205–212.
[87] H. Chen, M.C. Long, J. Xu, W.M. Cai, Chin. J. Catal. 27 (2006) 890–894.
[88] M.C. Long, W.M. Cai, Z.P. Wang, G.Z. Liu, Chem. Phys. Lett. 420 (2006) 71–76.
[89] R. Long, Y. Dai, B.B. Huang, Comput. Mater. Sci. 45 (2009) 223–228.
[90] K. Woan, G. Pyrgiotakis, W. Sigmund, Adv. Mater. 21 (2009) 2233–2239.
[91] D.M. Chen, Z.Y. Jiang, J.Q. Geng, J.H. Zhu, D. Yang, J. Nanoparticle Res. 11 (2009) 303–313.
[92] A. Tilocca, A. Selloni, J. Chem. Phys. 119 (2003) 7445–7450.
[93] K. Hashimoto, H. Irie, A. Fujishima, Jpn. J. Appl. Phys. Part 1-Regular Papers Brief Commun. Rev. Papers 44 (2005) 8269–8285.
[94] S.C. Padmanabhan, S.C. Pillai, J. Colreavy, S. Balakrishnan, D.E. McCormack, T.S. Perova, Y. Gun'ko, S.J. Hinder, J.M. Kelly, Chem. Mater. 19 (2007) 4474–4481.
[95] Y.L. Su, X.W. Zhang, S. Han, X.Q. Chen, L.C. Lei, Electrochem. Commun. 9 (2007) 2291–2298.
[96] P. Sampedro, G. Colón, M. Fernández-García, J. Photochem. Photobiol. A: Chem. 199 (2008) 136–143.